Variable-Band-Gap Poly(arylene ethynylene) Conjugated Polyelectrolytes Adsorbed on Nanocrystalline TiO_2: Photocurrent Efficiency as a Function of the Band Gap

Hui Jiang, Xiaoyong Zhao, Abigail H. Shelton, Seoung Ho Lee, John R. Reynolds, and Kirk S. Schanze*

Department of Chemistry, Center for Macromolecular Science and Engineering; University of Florida, P.O. Box 117200, Gainesville, Florida 32611-7200

ABSTRACT A series of poly(arylene ethynylene) conjugated polyelectrolytes (CPEs) substituted with carboxylic acid side groups have been synthesized and characterized. The polymers feature a backbone consisting of a carboxylated dialkoxyphenylene-1,4-ethynylene unit alternating with a second arylene ethynylene moiety of variable electron demand. The HOMO−LUMO gap is varied across the series, giving rise to a set of four polymers that have absorption maxima ranging from 404 to 495 nm. The CPEs adsorb effectively from solution onto nanostructured TiO_2 films, giving rise to TiO_2/CPE films that absorb ~90% of the incident light at the absorption band maximum. The photocurrent generation efficiency of the TiO_2/CPE films was examined in a solar cell configuration using an I_3^-/I^- propylene carbonate electrolyte and a Pt/fluorine-doped tin oxide counter electrode. Most of the films exhibit good photocurrent generation efficiency with a peak quantum efficiency of ~50% at wavelengths corresponding to the polymers' absorption band maximum. Interestingly, the photocurrent generation efficiency for the lowest-band-gap polymer is substantially lower compared to the other three systems. This effect is attributed to efficient nonradiative decay of excitons at trap sites arising from interchain contacts distal from the TiO_2/CPE interface.

KEYWORDS: conjugated polyelectrolyte • band gap • charge transfer • dye-sensitized solar cell • photocurrent generation • power conversion

INTRODUCTION

Conjugated polymers have been successfully used as active materials to construct a variety of electronic and electrooptical devices such as field-effect transistors (1, 2), light-emitting devices (3, 4), and solar cells (5−8). In order to tune the optical properties of conjugated polymers, various synthetic strategies have been employed, one of which is to introduce electron donor−acceptor interactions into the conjugated polymer backbone (9−11). Alternating copolymers containing adjacent repeat units with different electron demand (i.e., electron-poor/electron-rich) feature relatively low HOMO–LUMO (highest occupied molecular orbital−lowest unoccupied molecular orbital) band gaps. Consequently, these copolymers exhibit absorption and fluorescence at longer wavelength compared to structurally analogous homopolymers (9, 10). In a study reported previously, we utilized this strategy to prepare two series of variable-band-gap conjugated polyelectrolytes (CPEs), which feature a poly(phenylene ethynylene) backbone functionalized with anionic (sulfonate) and cationic (tetraalkylammonium) solubilizing groups (12). In this series, the conjugated backbone consists of a dialkoxyphenylene-1,4-ethynylene unit alternating with a second arylene ethynylene moiety, which has a different electron demand [1,4-phenyl (PPE), 2,5-thienyl (TH), 2,5-(3,4-ethylenedioxy)thienyl (EDOT), and 1,4-benzo[2,1,3]thiadiazole (BTD)] (12). This series of CPEs displays absorption maxima at wavelengths ranging from 400 to 550 nm and fluorescence maxima ranging from 440 to 600 nm (12). In addition, the study shows that the spectroscopic properties of the polymers are determined by the backbone structure; the nature of the side groups (i.e., whether they are cationic or anionic) have little effect on the absorption or emission wavelengths.

Since the pioneering work by O'Regan and Grätzel in 1991, which reported high-efficiency photoelectrochemical cells based on dye-sensitized nanocrystalline TiO_2 electrodes (13), dye-sensitized solar cells (DSSCs) have attracted considerable interest (14, 15). The sensitizer used in DSSCs is often a carboxy-substituted ruthenium polypyridine complex, although other metal complexes and organic dyes that are substituted with carboxylic acid units have been evaluated (16, 17). The carboxylic acid functional group is crucial to allowing the dye sensitizer to anchor onto the porous nanocrystalline TiO_2 surface (18, 19). Because of their high cross section for light absorption, tunable band gap, and the presence of multiple ionic side chains that can be used as anchoring groups, CPEs can also be used as effective light-harvesting and sensitizer materials for photoelectrochemical cells based on nanostructured TiO_2 electrodes. Indeed, in previous work, we and others have demonstrated that specific CPEs that are functionalized with carboxylic acid

* Corresponding author. Tel: 352-392-9133. Fax: 352-392-2395. E-mail: kschanze@chem.ufl.edu. Web site: http://chem.ufl.edu/~kschanze.
Received for review September 29, 2008 and accepted December 14, 2008

DOI: 10.1021/am800089n

Chart 1

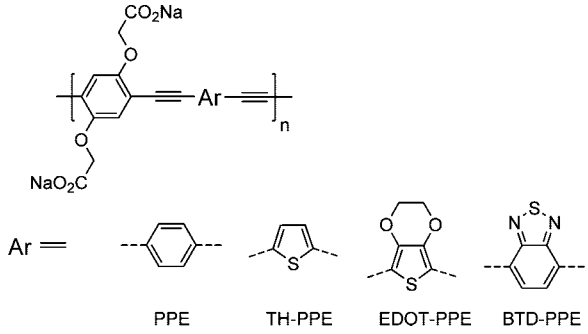

solubilizing groups can serve as effective sensitizers in DSSCs, with the cells exhibiting a relatively high incident photon-to-current efficiency (IPCE) and a moderate overall white-light power conversion efficiency (20–24).

We have an interest in the application of CPEs in solar cells, and on the basis of our prior work on variable-band-gap poly(phenylene ethynylene) CPEs, we recognize that it would be possible to use the same approach to vary the band gap of a series of carboxy-substituted polymers that could be used as sensitizers on nanocrystalline TiO_2. This would allow us to explore the relationship between light-harvesting and charge-injection efficiencies as a function of the band gap of the CPE sensitizer. Thus, in the present paper, we report the results of an investigation of the properties of photoelectrochemical cells constructed by using a series of carboxy-substituted poly(phenylene ethynylene) alternating copolymers in which the band gap is systematically varied by changing one of the repeat units in the conjugated backbone (Chart 1). This series of CPEs displays absorption maxima ranging from the blue into the mid-visible region, in direct analogy to the series of structurally analogous sulfonate- and ammonium-substituted CPEs that we reported previously (12). Each of the polymers adsorbs effectively onto nanocrystalline TiO_2 electrodes, presumably via interaction of the carboxyl group with the TiO_2 interface, giving rise to TiO_2/CPE films that absorb ≥90% of the incident light at the polymer's absorption maximum. As expected, the IPCE and overall power conversion efficiency exhibit a clear correlation with the polymer band gap, except for the polymer with the lowest band gap, BTD-PPE. The possible origin for the relatively poor performance for the BTD-PPE sensitizer is discussed.

EXPERIMENTAL SECTION

Materials and Synthesis. The approach used to synthesize PPE, TH-PPE, and EDOT-PPE (Chart 1) was identical with that described previously for the preparation of a series of 4-(trifluoromethyl)phenyl end-capped polymers with backbone structure identical with that of the parent polymer PPE (25). Details concerning the synthesis and characterization of all of the polymers are provided in the Supporting Information. Here we briefly summarize the process used. Polymers PPE, TH-PPE, and EDOT-PPE (Chart 1) were prepared via a precursor route (26), in which the carboxyl groups were protected as dodecyl esters. The dodecyl ester polymers were soluble in organic solvents and were characterized by high-resolution NMR and gel permeation chromatography. Subsequent to characterization, the ester groups were hydrolyzed with $(n\text{-Bu})_4N^+OH^-$ to afford the water-soluble CPEs. Attempts to prepare BTD-PPE via an analogous route failed because of reaction of the BTD-PPE backbone under the basic conditions used for hydrolysis of the dodecyl ester units. Thus, BTD-PPE was synthesized via a direct route (26) in which the CPE was prepared via polymerization of 2,2′-(2,5-diiodo-1,4-phenylene)bis(oxy)diacetate and 4,7-bis[(trimethylsilyl)ethynyl]benzo[*c*][1,2,5]thiadiazole in a mixed organic–aqueous solution (see the Supporting Information for details). After preparation and purification by dialysis, the CPEs were stored as aqueous stock solutions with a polymer repeat unit concentration of *ca.* 1 mM and pH ~ 8.

Prior to adsorption of the CPEs onto the TiO_2-coated electrodes, the polymers were protonated to the acid form by the addition of 3 N hydrochloric acid to an aliquot of the basic aqueous stock solution. The neutral CPEs (carboxylic acid form) precipitated from the solution. The precipitate was collected by centrifugation and then redissolved in dry *N*,*N*-dimethylformamide (DMF) (PPE, TH-PPE, and EDOT-PPE) or dimethyl sulfoxide (DMSO) (BTD-PPE) to afford a solution with a concentration of *ca.* 0.2 mg/mL.

Fluorine-doped tin oxide (FTO, TEC 8) glass substrates were purchased from Harford Glass (Harford, PA), and nanocrystalline TiO_2 paste (12% by weight; average particle size of about 13 nm) was purchased from Solaronix SA (Aubonne, Switzerland).

General Methods and Instrumentation. UV–visible absorption spectra were recorded with a Lambda 25 spectrophotometer from PerkinElmer. Steady-state fluorescence spectra were obtained with a Fluorolog-3 spectrofluorometer from Jobin Yvon. A 1-cm square quartz cuvette was used for all spectral measurements. Fluorescence quantum yields were measured relative to a Coumarin 102 standard (λ_{exc} = 380 nm and Φ_{em} = 0.67 in EtOH) (27). The cyclic voltammetry (CV) and differential pulse voltammetry (DPV) experiments were performed on a Bioanalytical Systems CW50 electrochemical analyzer at a scan rate of 50 mV/s. Measurements were carried out in nitrogen-degassed solutions with 0.1 M tetrabutylammonium hexafluorophosphate as the supporting electrolyte and ferrocene as the internal standard (0.43 V vs SCE in dry dichloromethane) (28). Nanosecond transient absorption spectra of dye-sensitized TiO_2 films were acquired with an experimental setup described previously (23, 29).

Photovoltaic Device Fabrication and Characterization. The photoelectrochemical cells were fabricated according to published procedures (23, 30). Briefly, TiO_2 paste was spread onto an FTO substrate, and the coated electrode was sintered at 450 °C for 30 min. The thickness of the sintered TiO_2 films was *ca.* 5 μm. The sintered electrode was immersed into the polymer solution for *ca.* 14 h to allow adsorption of the polymer onto the TiO_2 film. To complete the photoelectrochemical cell, an FTO substrate that had a thin Pt film (5 nm) that was deposited by sputtering was used as the counter electrode, and the electrolyte solution consisted of propylene carbonate containing 0.05 M I_2 and 0.5 M LiI. The working cell was fabricated by sandwiching a thin film of the electrolyte solution between the active (TiO_2/FTO) and counter (Pt/FTO) electrodes, and the assembly was held together using a mini binder clip.

The current–voltage characteristics of the photoelectrochemical cells were measured with a Keithley SMU 2400 source meter under AM1.5 (100 mW/cm^2) illumination provided by a 150 W Xe arc lamp (Oriel Instruments, Stratford, CT). For IPCE measurements, cells were illuminated by monochromatic light from an Oriel Cornerstone 130 $^1/_8$ m spectrometer, and the current response under short-circuit condition was recorded at 10-nm intervals using a Keithley SMU 2400 source meter. The intensity of the light source at each wavelength was determined by using an energy meter (S350, UDT Instruments, San Diego, CA) equipped with a calibrated silicon detector (model 221, UDT

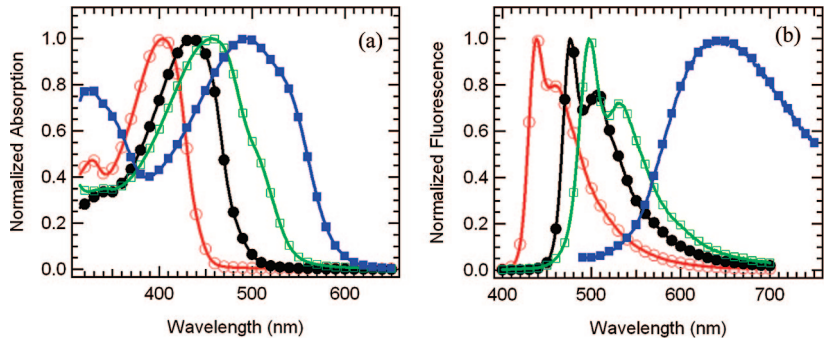

FIGURE 1. Normalized absorption (a) and fluorescence (b) of studied CPEs in methanol: (○) PPE; (●) TH-PPE; (□) EDOT-PPE; (■) BTD-PPE.

Table 1. Photophysical Properties of CPEs in a Methanol Solution

	λ_{max}^{ab}(nm)	λ_{max}^{em}(nm)	Φ_{em}
PPE	404	438	0.17
TH-PPE	435	476	0.13
EDOT-PPE	457	497	0.09
BTD-PPE	495	642	0.002

Instruments, San Diego, CA). The active area of the photoelectrochemical cells was *ca.* 1.0 cm^2, and in all of the efficiency measurements, the cells were illuminated through the TiO_2/FTO electrode.

RESULTS AND DISCUSSION

Optical Properties of CPEs in a Methanol Solution. The absorption and fluorescence spectra of the series of four carboxylate-substituted CPEs (as the sodium salts) were examined in a methanol solution. The spectra are illustrated in Figure 1, and the wavelength maxima and fluorescence quantum yields are listed in Table 1. The wavelength maxima of the absorption and fluorescence spectra systematically red-shift across the series in the order PPE < TH-PPE < EDOT-PPE < BTD-PPE, with the absorption maxima ranging from 404 nm (PPE) to 495 nm (BTD-PPE). As can be seen from the data in Table 1, the fluorescence quantum yields decrease along the series PPE > TH-PPE > EDOT-PPE ≫ BTD-PPE, with a clear trend that the quantum yield decreases with the CPE band gap. The absorption and fluorescence band shapes, along with the general trends in the absorption and emission wavelengths and fluorescence quantum yields observed for the present series of CPEs, are very similar to those reported previously for the two series of sulfonate- and ammonium-substituted CPEs with the same backbone structure (12). This feature underscores the fact that the optical properties of the polymers are determined by the molecular and electronic structure of the conjugated backbone, with the ionic side groups playing the role of determining the solution (and aggregation) properties of the materials.

The red shift in the absorption and fluorescence spectra across the series arises because the HOMO−LUMO band gap decreases in the order PPE > TH-PPE > EDOT-PPE > BTD-PPE. In the case of TH-PPE and EDOT-PPE, the band-gap narrowing likely arises mainly because of an increase in the HOMO level caused by incorporation of the thienylene and ethylene dioxythienylene repeat units (31, 32). However, for

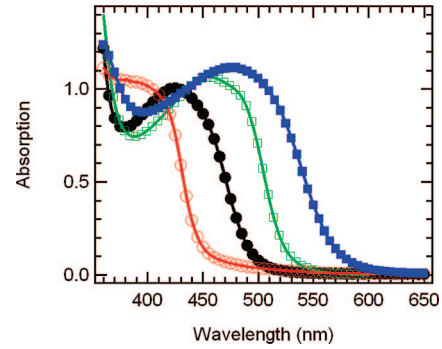

FIGURE 2. Absorption of CPE-sensitized TiO_2 films: (○) PPE; (●) TH-PPE; (□) EDOT-PPE; (■) BTD-PPE.

BTD-PPE, which has the lowest band gap of the series, the HOMO−LUMO gap narrowing likely arises because the BTD moiety is a strong electron acceptor, leading to lowering of the LUMO level (31, 32). In this polymer, there is likely a degree of donor−acceptor character in the backbone, where the dialkoxyphenylene unit acts as a donor and the BTD unit acts as an acceptor. The existence of donor−acceptor character in BTD-PPE is reflected by several features. First, the fluorescence of this polymer is Stokes-shifted to a significantly larger extent compared to the other CPEs. In addition, the polymer's fluorescence spectrum is broad and structureless. Each of these features is typical for chromophores that undergo a significant change in the dipole moment (due to charge transfer) upon photoexcitation (33, 34). Another feature of note is the fact that the fluorescence quantum yield for BTD-PPE is significantly less than that for the other CPEs. While the low quantum yield may arise in part because of the energy gap law (35), on the basis of previous studies, we believe that the low fluorescence yield is largely due to quenching of the excitons by interchain interactions, which have a significant degree of charge-transfer character (exciplex). This effect was noted in our previous study of the sulfonate- and ammonium-substituted CPEs, where low fluorescence quantum yields were also observed for BTD-containing polymers (12). This feature will be further discussed later in the context of the photocurrent efficiency for BTD-PPE films on TiO_2 electrodes.

Absorption and Transient Absorption Spectra of CPE-Sensitized TiO_2 Films. Figure 2 shows the absorption spectra of TiO_2 films after 14 h of immersion in DMF or DMSO solutions of the acid forms of the CPEs. Not surprisingly, the spectra appear as a superposition of the

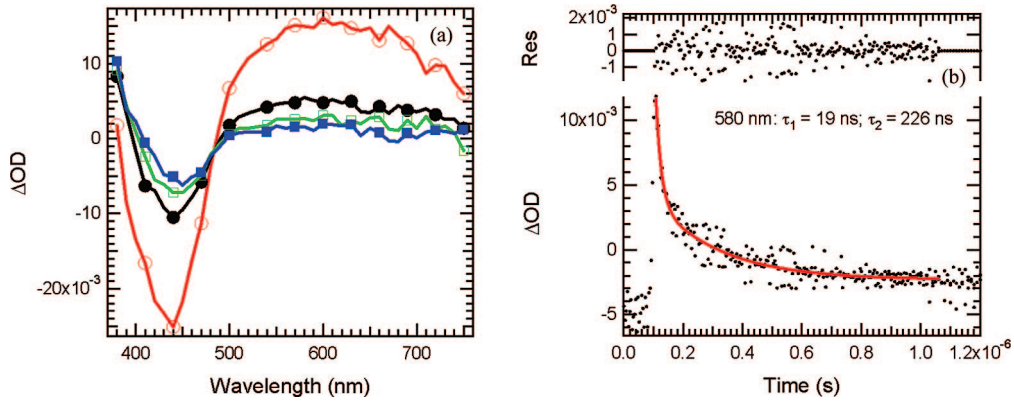

FIGURE 3. Transient absorption spectra (a) and decay kinetics monitored at 580 nm (b) of a TH-PPE-sensitized TiO_2 film following 355-nm laser excitation: (○) 0 ns; (●) 40 ns; (□) 80 ns; (■) 120 ns.

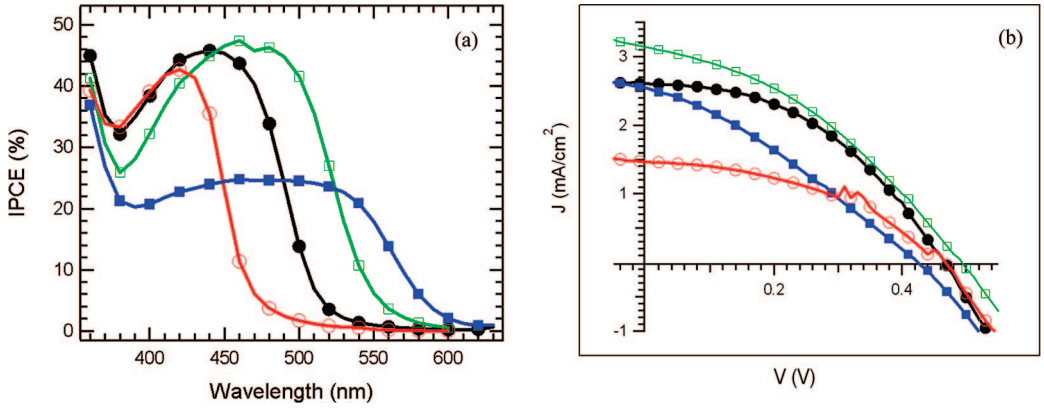

FIGURE 4. (a) Photocurrent action spectra of CPE-sensitized solar cells and (b) $J-V$ characteristics of CPE-sensitized solar cells under AM1.5 conditions: (○) PPE; (●) TH-PPE; (□) EDOT-PPE; (■) BTD-PPE.

absorption spectra of the CPEs in MeOH with the absorption of TiO_2 (which absorbs below 380 nm). Importantly, the absorption band position and band shape of the CPEs are essentially unchanged by adsorption on TiO_2. The absorption data clearly show that in the acid form the CPEs are able to effectively adsorb onto the nanostructured TiO_2 interface, giving rise to films that effectively absorb 90% or more of the incident light at the absorption band maxima. Photoluminescence studies of the TiO_2/CPE films show that the emission is strongly quenched by the semiconductor, presumably by charge injection.

Nanosecond transient absorption studies were carried out with the CPE-modified TiO_2 films in order to investigate whether photoexcitation leads to effective charge injection. In each case, similar results were observed, so here we present only the data for the TiO_2/TH-PPE film. As shown in Figure 3, excitation of the film at 355 nm (~5 ns pulse; 3 mJ energy) leads to a strong transient absorption difference spectrum characterized by ground-state bleaching in the 400−500 nm region, combined with broad absorption at $\lambda > 500$ nm with a band maximum at ~600 nm. The transient absorption is ascribed to the radical-cation state of TH-PPE (positive polaron), which is produced during the laser pulse by photoinduced charge injection into the TiO_2 conduction band (36). The transient absorption decays with multiexponential kinetics, with a substantial fraction of the signal decaying within 500 ns of excitation, with the decay being ascribed to charge recombination. The charge recombination kinetics that are observed with the TiO_2/CPE films are comparable to those seen for small-molecule metal complex and organic dye sensitizers (19, 37, 38). The transient absorption data provide clear evidence that photoexcitation of the TiO_2/CPE films leads to efficient charge injection.

Solar Cell Characterization. The response of photoelectrochemical cells constructed using the TiO_2/CPE films was evaluated. The cells were evaluated with the films immersed in an I_3^-/I^- solution in propylene carbonate with a Pt/FTO counter electrode. Parts a and b of Figure 4 illustrate respectively the photocurrent action (ICPE) spectra obtained under monochromatic illumination and the current density−voltage ($J-V$) response of the cells under AM1.5 (100 mW/cm^2) simulated solar illumination. First, the IPCE spectra for the TiO_2/PPE, TiO_2/TH-PPE, and TiO_2/EDOT-PPE films are in qualitative agreement with the absorption spectra of the films (compare Figure 4a with Figure 2). In each case, the peak quantum efficiency is ~45%, with the maximum shifting to the red along the series PPE < TH-PPE < EDOT-PPE, consistent with the trend in the absorption spectra. The results suggest that charge injection is relatively efficient for each of the three polymers. However, while the IPCE spectrum for the TiO_2/BTD-PPE film is shifted further

Table 2. Solar Cell Characteristics under AM1.5 Illumination

film	IPCE (%)	J_{sc} (mA/cm^2)	V_{oc} (V)	FF (%)	η (%)
TiO_2/PPE	42.7 @420 nm	1.46	0.47	49.2	0.34
TiO_2/TH-PPE	45.8 @440 nm	2.60	0.47	43.4	0.53
TiO_2/EDOT-PPE	47.4 @460 nm	3.12	0.50	37.2	0.58
TiO_2/BTD-PPE	24.7 @480 nm	2.52	0.43	30.5	0.33

to the red (consistent with the absorption of BTD-PPE), the IPCE spectrum is much broader and the peak quantum efficiency is only ~25%. This result suggests that for some reason charge injection is considerably less efficient in the TiO_2/BTD-PPE system.

The $J-V$ characteristics for the CPE-sensitized cells are shown in Figure 4b, and the performances of the cells in terms of short-circuit current (J_{sc}), open-circuit voltage (V_{oc}), fill factor (FF), and power conversion efficiency (η) are summarized in Table 2, along with the maximum IPCE values. Interestingly, in accordance with the IPCE results, J_{sc} and η increase along the series TiO_2/PPE < TiO_2/TH-PPE < TiO_2/EDOT-PPE. This trend is consistent with the fact that across this series the absorption maximum of the CPEs shifts to the red, leading to improved matching of the absorption with the solar spectrum and, consequently, increased photocurrent and power conversion efficiency. There is a slight falloff in the fill factor across the series, which likely arises because of the effect of cell resistance coupled with the increased current density. However, for the TiO_2/BTD-PPE films, consistent with the IPCE data, the J_{sc} and η values are significantly lower compared to those of the other CPEs. The considerably lower AM1.5 efficiency seen for the TiO_2/BTD-PPE system again points to the fact that for some reason charge injection is less efficient compared to that for the other CPEs.

Why Is Charge Injection Inefficient in the TiO_2/BTD-PPE System? As discussed above, the TiO_2/BTD-PPE-based solar cell exhibits substantially lower photocurrent generation efficiency compared to the other three TiO_2/CPE systems. Several reasons can be considered to explain the difference. First, it is important to consider the possibility that, because the BTD-PPE singlet excited state is lower in energy compared to the other CPEs, charge injection may be inefficient because the process is not sufficiently exothermic. In order to provide an estimate for the driving force for charge injection, CV and DPV were performed on the CPEs in solution. (Voltammetry was performed with the CPEs in their ester precursor form in dichloromethane, except for BTD-PPE, which was measured in DMSO.) Unfortunately, in each case the anodic branch of the CV did not provide a response; however, it was possible to obtain quasi-reversible waves for reduction of the polymers, and the onset potentials are −1.12, −1.12, −0.87, and −1.02 V (vs SCE) for PPE, TH-PPE, EDOT-PPE, and BTD-PPE, respectively. In the absence of oxidation potentials, it is only possible to use the ground-state reduction potentials as estimates for the excited-state oxidation potentials of the CPEs. (This assumption neglects the Coulomb binding energy in the singlet excited state, which is typically ≤0.3 eV.) The important point is that the electrochemistry suggests that for each of the CPEs (including BTD-PPE) charge injection into TiO_2 is thermodynamically favorable, given that the estimated excited-state oxidation potentials are considerably more negative than the conduction band of TiO_2, which is estimated to be −0.42 V vs SCE (39). Given this result, it is reasonable to conclude that the lower efficiency for the TiO_2/BTD-PPE system is not due to an insufficient thermodynamic driving force for charge injection (32, 40).

Scheme 1. Trapping of Excitons by a Charge-Transfer State for the TiO_2/BTD-PPE Film[a]

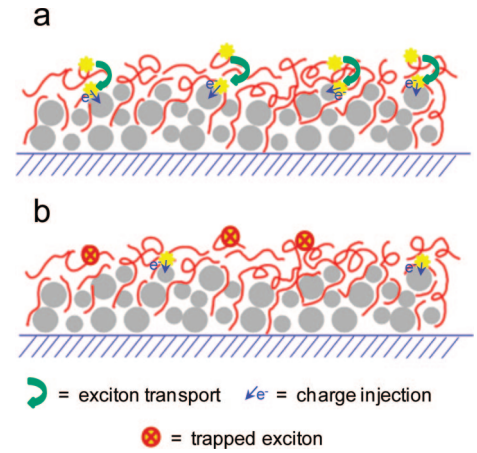

[a] (a) Excitons generated distal from the interface are transported to the interface to undergo charge injection. (b) Excitons generated distal from the interface are trapped by aggregate states.

A second possible reason for inefficient photocurrent generation in the TiO_2/BTD-PPE system is that there is an active nonradiative decay pathway that effectively competes with charge injection. In order to understand this point, we refer to Scheme 1, which illustrates a model for the structure of the interface between the adsorbed CPEs and the nanostructured TiO_2. As shown in this scheme, it is very likely that the CPEs adsorb onto the TiO_2 surface, giving rise to a complex interfacial structure where some polymer segments are in close proximity to the surface (<10 Å) and others are relatively distant (>30 Å) because of "loops or kinks" in the polymer chains or because of adsorption of aggregates from solution. [Atomic force microscopy (AFM) studies carried out to compare the morphology of TiO_2 and TiO_2/PPE surfaces do not provide clear evidence for the existence of polymer aggregates on the surface; see Figure S1 in the Supporting Information. However, the surface of the nanostructured films is complex, which limits the spatial resolution that could be attained by AFM.] Despite this complex interface structure, the fact that charge injection is relatively efficient (~45% IPCE) for the TiO_2/PPE, TiO_2/TH-PPE and TiO_2/EDOT-PPE systems suggests that singlet excitons that are generated on polymer segments that are distal from the surface are able to diffuse efficiently to the TiO_2 interface for charge injection. In other words, in these systems the CPEs are effectively able to act as light-harvesting arrays, effectively absorbing and channeling excitons to the interface for charge separation (41−43).

The lower photocurrent efficiency observed in the TiO_2/BTD-PPE system suggests that, in this case, excitons that are produced distant from the TiO_2 surface are trapped and/or quenched before they are able to diffuse to the interface to undergo charge injection. The quenching process likely involves the formation of interchain states having charge-transfer character; this state acts as a trap, localizing the excitons and facilitating their nonradiative decay. In support of this idea, in a previous study, we examined the photophysics of a pair of cationic and anionic CPEs with the same backbone structure as BTD-PPE (12). For both the cationic and anionic CPEs, it was observed that under conditions where the polymers are aggregated the fluorescence of the singlet exciton is strongly quenched. The quenching was ascribed to the formation of an "exciplex-like" state arising from charge transfer between polymer segments that are brought into close proximity (possibly via $\pi-\pi$ interactions) in the aggregate.

SUMMARY AND CONCLUSIONS

A series of poly(arylene ethynylene) CPEs substituted with carboxylic acid side groups have been synthesized and adsorbed onto nanocrystalline TiO_2. The polymers feature a backbone consisting of a carboxylated dialkoxyphenylene-1,4-ethynylene unit alternating with a second arylene ethynylene moiety of variable electron demand. The HOMO−LUMO gap varies across the series, giving rise to a set of four polymers that have absorption maxima ranging from 404 to 495 nm. Immersion of nanocrystalline TiO_2 films into DMF or DMSO solutions containing the CPEs (in their acid form) leads to adsorption of the polymers onto the semiconductor surface with coverage sufficient to give rise to >90% light absorption at wavelengths corresponding to the polymers' band maximum. The TiO_2/CPE films were evaluated in a DSSC configuration using an I_3^-/I^- propylene carbonate electrolyte and a Pt/FTO counter electrode. Each of the films exhibits a significant photocurrent under monochromatic and white-light (AM1.5) illumination. For each CPE, the photocurrent action spectrum matches the absorption spectra well, and the IPCE reaches approximately 50% at the absorption band maximum for the PPE, TH-PPE, and EDOT-PPE systems. The photocurrent and power conversion efficiency under AM1.5 illumination increase in the order PPE < TH-PPE < EDOT-PPE, consistent with a red shift in the polymers' absorption. Interestingly, the IPCE and power conversion efficiency for the TiO_2/BTD-PPE system are substantially less than those for the other CPEs, and the decreased efficiency is attributed to exciton trapping in polymer aggregates that are present in the film but separated from the TiO_2 interface. The relatively good photocurrent efficiency observed for the other CPEs suggests that these polymers can act as effective light-harvesting elements, with excitons that are produced distal from the TiO_2 CPE interface being efficiently channeled to the semiconductor surface where charge injection can occur.

Acknowledgment. We acknowledge the United States Department of Energy, Office of Basic Energy Sciences (Grant DE-FG-02-96ER14617), for support of this work.

Supporting Information Available: CPE synthesis and characterization and AFM images of TiO_2 and TiO_2/PPE films. This material is available free of charge via the Internet at http://pubs.acs.org.

REFERENCES AND NOTES

(1) Dimitrakopoulos, C. D.; Malenfant, P. R. L. *Adv. Mater.* **2002**, *14*, 99–117.
(2) Garnier, F. *Acc. Chem. Res.* **1999**, *32*, 209–215.
(3) Burroughes, J. H.; Bradley, D. D. C.; Brown, A. R.; Marks, R. N.; Mackay, K.; Friend, R. H.; Burns, P. L.; Holmes, A. B. *Nature* **1990**, *347*, 539–541.
(4) Mitschke, U.; Bauerle, P. *J. Mater. Chem.* **2000**, *10*, 1471–1507.
(5) Sariciftci, N. S.; Smilowitz, L.; Heeger, A. J.; Wudl, F. *Science* **1992**, *258*, 1474–1476.
(6) Yu, G.; Gao, J.; Hummelen, J. C.; Wudl, F.; Heeger, A. J. *Science* **1995**, *270*, 1789–1791.
(7) Gunes, S.; Neugebauer, H.; Sariciftci, N. S. *Chem. Rev.* **2007**, *107*, 1324–1338.
(8) Roncali, J.; Leriche, P.; Cravino, A. *Adv. Mater.* **2007**, *19*, 2045–2060.
(9) Hou, J. H.; Yang, C. H.; Qiao, J.; Li, Y. F. *Synth. Met.* **2005**, *150*, 297–304.
(10) Li, X. Z.; Zhang, Y.; Yang, R. Q.; Huang, J.; Yang, W.; Cao, Y. *J. Polym. Sci., Part A: Polym. Chem.* **2005**, *43*, 2325–2336.
(11) Kitamura, C.; Saito, K.; Nakagawa, M.; Ouchi, M.; Yoneda, A.; Yamashita, Y. *Tetrahedron Lett.* **2002**, *43*, 3373–3376.
(12) Zhao, X.; Pinto, M. R.; Hardison, L. M.; Mwaura, J.; Muller, J.; Jiang, H.; Witker, D.; Kleiman, V. D.; Reynolds, J. R.; Schanze, K. S. *Macromolecules* **2006**, *39*, 6355–6366.
(13) O'Regan, B.; Grätzel, M. *Nature* **1991**, *353*, 737–740.
(14) Grätzel, M. *Prog. Photovoltaics* **2006**, *14*, 429–442.
(15) Robertson, N. *Angew. Chem., Int. Ed.* **2006**, *45*, 2338–2345.
(16) Hara, K.; Miyamoto, K.; Abe, Y.; Yanagida, M. *J. Phys. Chem. B* **2005**, *109*, 23776–23778.
(17) Grätzel, M. *J. Photochem. Photobiol. A* **2004**, *164*, 3–14.
(18) Argazzi, R.; Bignozzi, C. A.; Heimer, T. A.; Castellano, F. N.; Meyer, G. *J. Inorg. Chem.* **1994**, *33*, 5741–5749.
(19) Hagfeldt, A.; Grätzel, M. *Acc. Chem. Res.* **2000**, *33*, 269–277.
(20) Kim, Y.-G.; Walker, J.; Samuleson, L. A.; Kumar, J. *Nano Lett.* **2003**, *3*, 523–525.
(21) Liu, J.; Kadnikova, E. N.; Liu, Y.; McGehee, M. D.; Frechet, J. M. J. *J. Am. Chem. Soc.* **2004**, *126*, 9486–9487.
(22) Liu, Y.; Summers, M. A.; Edder, C.; Frechet, J. M. J.; McGehee, M. D. *Adv. Mater.* **2005**, *17*, 2960–2964.
(23) Mwaura, J. K.; Zhao, X.; Jiang, H.; Schanze, K. S.; Reynolds, J. R. *Chem. Mater.* **2006**, *18*, 6109–6111.
(24) Liu, X.; Zhu, R.; Zhang, Y.; Liu, B.; Ramakrishna, S. *Chem. Commun.* **2008**, 3789–3791.
(25) Zhao, X.; Jiang, H.; Schanze, K. S. *Macromolecules* **2008**, *41*, 3422–3428.
(26) Schanze, K. S.; Zhao, X. In *Handbook of Conducting Polymers*, 3rd ed.; Skotheim, T. A., Reynolds, J. R., Eds.; CRC Press LLC: Boca Raton, FL, 2007; pp 14.1−14.29.
(27) Jones, G.; Jackson, W. R.; Choi, C.; Bergmark, W. R. *J. Phys. Chem.* **1985**, *89*, 294–300.
(28) Jones, N. D.; Wolf, M. O.; Giaquinta, D. M. *Organometallics* **1997**, *16*, 1352–1354.
(29) Wang, Y.; Schanze, K. S. *Chem. Phys.* **1993**, *176*, 305–319.
(30) Nazeeruddin, M. K.; Kay, A.; Rodicio, I.; Humphry-Baker, R.; Muller, E.; Liska, P.; Vlachopoulos, N.; Grätzel, M. *J. Am. Chem. Soc.* **1993**, *115*, 6382–6390.
(31) Karikomi, M.; Kitamura, C.; Tanaka, S.; Yamashita, Y. *J. Am. Chem. Soc.* **1995**, *117*, 6791–6792.
(32) Blanchard, P.; Raimundo, J. M.; Roncali, J. *Synth. Met.* **2001**, *119*, 527–528.
(33) In ongoing work, we have studied the solvent dependence of the fluorescence of a CPE with the same backbone structure as BTD-PPE but with branched side groups. The fluorescence spectrum of this polymer red-shifts as the solvent polarity increases in

methanol/water mixtures. This result is consistent with the fluorescent state having charge-transfer character (34).
(34) Lee, S. H.; Zhao, X.; Jiang, H.; Moriena, G.; Komurlu, S.; Kleiman, V. D.; Schanze, K. S., manuscript in preparation.
(35) Caspar, J. V.; Meyer, T. J. *J. Phys. Chem.* **1983**, *87*, 952–957.
(36) A transient absorption experiment carried out with 435-nm excitation of the TH-PPE/TiO_2 film produced essentially the same transient absorption spectrum; however, the transient absorption signal was weaker because of the fact that the laser power was limited to 500 μJ at 435 nm.
(37) Hagfeldt, A.; Grätzel, M. *Chem. Rev.* **1995**, *95*, 49–68.
(38) Kalyanasundaram, K.; Grätzel, M. *Coord. Chem. Rev.* **1998**, *177*, 347–414.
(39) Palomares, E.; Clifford, J. N.; Haque, S. A.; Lutz, T.; Durrant, J. R. *J. Am. Chem. Soc.* **2003**, *125*, 475–482.
(40) It is also unlikely that iodide oxidation is less efficient for BTD-PPE relative to the other polymers. This is because the ground-state oxidation potential for this polymer is more positive compared to the other polymers because of the electron-withdrawing effect of the BTD unit on the HOMO of the polymer; see ref 41.
(41) Levitsky, I. A.; Kim, J.; Swager, T. M. *J. Am. Chem. Soc.* **1999**, *121*, 1466–1472.
(42) Mikhnenko, O. V.; Cordella, F.; Sieval, A. B.; Hummelen, J. C.; Blom, P. W. M.; Loi, M. A. *J. Phys. Chem. B* **2008**, *112*, 11601–11604.
(43) Scully, S. R.; McGehee, M. D. *J. Appl. Phys.* **2006**, *100*, 34907.1−34907.5.

AM800089N